Journal of Catalysis **186,** 169–180 (1999)
Article ID jcat.1999.2553, available online at http://www.idealibrary.com on IDEAL®

Sulfur Deactivation of Fatty Ester Hydrogenolysis Catalysts

D. S. Brands, G. U-A-Sai, E. K. Poels,[1] and A. Bliek

Department of Chemical Engineering, University of Amsterdam, Nieuwe Achtergracht 166, 1018 WV, Amsterdam, The Netherlands

Received January 22, 1999; revised April 12, 1999; accepted April 12, 1999

Trace organosulfur compounds present as natural impurities in oleochemical feedstocks may lead to deactivation of copper-containing catalysts applied for hydrogenolysis of esters toward fatty alcohols. In this paper, the sulfur deactivation of Cu/SiO_2 and $Cu/ZnO/SiO_2$ catalysts was studied in the liquid-phase hydrogenolysis of methyl palmitate. The rate of deactivation is fast and increases as a function of the sulfur-containing compound present: octadecanethiol ≈ dihexadecyl disulfide < benzyl isothiocyanate < methyl *p*-toluene sulfonate < dihexadecyl sulfide < dibenzothiophene. The rapid deactivation is caused by the fact that sulfur is quantitatively removed from the reaction mixture and because mainly surface sulfides are formed under hydrogenolysis conditions. The life time of a zinc-promoted catalyst is up to two times higher than that of the Cu/SiO_2 catalyst, most likely due to zinc surface sulfide formation. The maximum sulfur coverage obtained after full catalyst deactivation with dibenzothiophene and dihexadecyl sulfide—the sulfur compounds that cause the fastest deactivation—may be as low as 0.07. This is due to the fact that decomposition of these compounds as well as the hydrogenolysis reaction itself proceeds on ensembles of copper atoms. For the most reactive sulfur compounds, surface coverage near the maximum value of $\theta_{Cu} = 0.5$ or—in the presence of zinc—formally in excess of this quantity may be reached at full catalyst deactivation. At that point, still some sulfur uptake occurs. Decomposition of such compounds is even possible in the absence of hydrogen and sulfur is not laid down in a dispersed fashion, as in the case of dibenzothiophene and dihexadecyl sulfide. Catalyst regeneration studies reveal that activity cannot be regained by reduction or combined oxidation/reduction treatments. XRD, TPR, and TPO results confirm that no distinct bulk copper or zinc sulfide or sulfate phases are present.

Key Words: **copper catalysts; zinc-promoted; silica-supported; ester hydrogenolysis; methyl palmitate; sulfur deactivation; deactivation mechanism.**

INTRODUCTION

The hydrogenolysis of fatty methyl esters is a step in the preparation of fatty alcohols from natural fats and oils. Industrially, copper–chromium catalysts are used for this reaction (1). Since the chromium component of this catalyst is under discussion for environmental reasons (2), research is focused on the replacement of chromium by other promoters like manganese and zinc (3–5). We have shown that $Cu/ZnO/SiO_2$ and $Cu/MnO/SiO_2$ catalysts are active in the ester hydrogenolysis reaction and that these catalysts, when properly pretreated, are more active than industrial copper–chromium catalysts both on a catalyst volume or weight basis (5, 6).

Impurities in Fatty Ester Feedstocks

In natural fatty methyl ester feedstocks, originating mainly from coconut, palm, and palm kernel oil, impurities such as chlorine-, nitrogen-, phosphorus-, and sulfur-containing compounds (7) and free fatty acids (1, 8) are present, all acting as catalyst poisons.

Sulfur is known to strongly deactivate copper catalysts in ester hydrogenolysis (7) and also the sulfur content of, e.g., synthesis gas during methanol synthesis should be below 0.1 ppm (7, 9). Such a low sulfur content is unattainable in methyl ester feedstocks. As a rule of thumb, 1 kg of copper catalyst per ppm of sulfur is required for the production of 1 metric ton of fatty alcohols.

Little is known about the nature of the sulfur compounds present in fatty methyl ester feedstocks prepared from natural fats and oils. Possible candidates are degradation products of sulfur-containing proteins (like thiols and sulfides) and glucosynolates (10–12). The main sulfur-containing products of both thermal and enzymatic degradation of glucosynolates are isothiocyanates (*R*–N=C=S) (10–13). Olive oil reportedly contains measurable quantities of 4-methoxy-2-methyl-2-butanethiol (14). For rapeseed oil, isothiocyanates, hydrogen sulfide, methanethiol, carbon disulfide, and dimethyl sulfide were identified (12, 15).

Sulfur could also originate from the acids used as a catalyst for the preparation of methyl esters from fatty acids (16). Examples are *p*-toluenesulfonic acid, methanesulfonic acid, and sulfuric acid (16–18).

The Nature of the Sulfur–Metal Interaction

Numerous studies have been performed on the deactivation of copper-containing methanol synthesis catalysts with different sulfur-containing compounds like COS, H_2S, and

[1] To whom correspondence should be addressed. Fax: +31-20-5255604. E-mail: poels@its.chem.uva.nl.

0021-9517/99 $30.00

thiophene (10, 19, 20–24). Deactivation studies of copper-containing Fischer-Tropsch (25), hydrocarbon and carbon monoxide oxidation (26, 27), methanation (28), fat hydrogenation (29, 30), and water–gas shift (31) catalysts have also been carried out. All studies report deactivation upon the addition of small quantities of sulfur compounds.

The severity of the deactivation of non-noble-metal catalysts induced by sulfur is caused by the strong metal–sulfur bond. The free energy of the formation of bulk Cu_2S is -122.1 kJ mol^{-1} at 298 K (for $2Cu + \frac{1}{2}S_2 \rightarrow Cu_2S_{bulk}$ (32)). This implies that bulk sulfides of copper may be formed at very low concentrations of the sulfur-containing molecule. The heat of adsorption of sulfur on most copper crystal faces is about -170 kJ mol^{-1} (for $2Cu + \frac{1}{2}S_2 \rightarrow Cu_2S_{surface}$) while the heat of formation of bulk copper sulfide is about -140 kJ mol^{-1} (for $2Cu + \frac{1}{2}S_2 \rightarrow Cu_2S_{bulk}$ (33)). This—and the fact that the rate-determining step of bulk copper sulfide formation is the solid state diffusion of sulfur in copper (or vice versa)—implies that preferentially surface sulfides are formed. The formation of surface sulfides at H_2S concentrations that lie well below the limit required for the formation of stable bulk sulfides is well known for both nickel and copper catalysts (34, 35). The difference in exothermicity between surface and bulk sulfidation of copper, however, is not as large as that found for nickel, so concurrent surface and bulk sulfidation of copper catalysts is more likely. This obviously has severe implications for the deactivation rate during industrial application. The maximum surface coverage of sulfur on most copper crystal planes is about 0.5, although for some rough planes a surface coverage of up to 1.0 was found (33, 36).

Since the free energy of formation of bulk ZnS (-146 kJ mol^{-1} at 298 K, for $Zn + \frac{1}{2}S_2 \rightarrow ZnS_{bulk}$ (32)) is lower than that of Cu_2S, some form of protection is expected from the presence of zinc in the catalyst (34). Zinc oxide is, for instance, used as a sulfur trap prior to steam reforming (37), absorbing sulfur at 100–400°C in a stoichiometry up to 4 : 1 (Zn : S) and cannot be regenerated (38).

Deactivation Mechanisms

Sulfur adsorption on non-noble-metal catalysts may cause deactivation of the active phase in at least four different ways (11, 33):

- Blocking of active sites and thereby inhibiting the adsorption of reactants. This could be due to either adsorbed sulfur itself and/or the remainder of the (organic) sulfur-containing molecule. Maxted, in studying the effect of sulfides on metallic catalysts, reports that their toxicity depends on the length of the alkyl chain, up to approximately eight carbon atoms (39).
- When a (side) reaction requires an ensemble of active sites, the coverage of only a part of the active surface in a structured fashion may lead to a substantial decrease in the rate of this reaction. This may result in increased selectivity for hydrogenation reactions (40–42)).
- Changing the active material (electronically) so centers with different catalytic properties are formed. Some authors suggest the electronic effects to be the main sulfur deactivation mechanism for nickel methanation catalysts (43, 44).
- Sulfur may cause an increase in surface self-diffusion (surface mobility), thus reducing catalytic activity by sintering or restructuring of the active metal.

Catalyst Regeneration

Regeneration of sulfur-poisoned base metal catalysts is problematic, due to the low free energy of formation of the metal sulfides and surface sulfides. Most literature on regeneration procedures is dedicated to sulfur-deactivated nickel catalysts ((34, 45) and references therein). Examples are treatments under hydrogen, oxygen, air, and/or steam (46) as well as oxidation–reduction cycles (47, 48). Bonzel (49) reports that a sulfur-covered Cu(110) surface can be regenerated by applying a treatment in oxygen above 873 K. Regeneration of a sulfur-covered Cu(111) surface using a hydrogen treatment is reported to proceed only at a very slow rate (31). In the patent literature, procedures to remove organic and inorganic residues of spent ester hydrogenation catalysts include washing with solvents, treatment with acids, and high-temperature treatment in oxygen and/or a vacuum (50, 51). The operating temperature is limited by the fact that the procedure should not cause active metal sintering or phase transitions of the catalyst carrier.

Sulfur Compounds Tested

To establish the industrial applicability of the Cu/ZnO/SiO_2 catalyst system and the low-pressure liquid-phase process developed earlier in our laboratory (52), the influence of various sulfur compounds in the ester feed on catalyst activity was examined. The unpromoted Cu/SiO_2 catalyst is used as a reference. On the basis of the sulfur-containing molecules that were identified and expected in natural fats, oils, and methyl esters as discussed above, the following model sulfur compounds were selected: octadecanethiol (coded as $C_{18}SH$), dihexadecyl sulfide ($C_{16}SC_{16}$), dihexadecyl disulfide ($C_{16}S_2C_{16}$), dibenzothiophene (DBT), and benzyl isothiocyanate (ITCN). *p*-Toluenesulfonic acid was not sufficiently soluble in our reaction medium (octane), so the methyl ester of this compound was used (MePTSA). An additional advantage of using the ester instead of the acid is the fact that the influence of the acid group of *p*-toluenesulfonic acid is now eliminated. Additionally, hexadecanethiol ($C_{16}SH$) instead of octadecanethiol was used in some mechanistic experiments.

EXPERIMENTAL

Chemicals

1-Octadecanethiol (Aldrich, 98% pure) and 1-hexadecanethiol (Aldrich, 92% pure) were purified by vacuum distillation to >99.5% purity (determined by GC analysis) before use. Dihexadecyl sulfide was prepared according to a method described in (53). Dihexadecyl disulfide was prepared by refluxing hexadecanethiol under an atmosphere of ambient air. Both sulfides were recrystallized and vacuum-distilled to obtain a >99.5% purity. Dibenzothiophene (Aldrich, 99% pure), methyl *p*-toluenesulfonate (Merck, 98% pure), benzyl isothiocyanate (Aldrich, 98% pure), octane (Janssen, 98.5% pure), and octadecane (Merck, 98% pure) were used without further purification. Methyl palmitate (the methyl ester of hexadecanoic acid) was prepared by a method described in (54). A purity of 99.95% (determined by titration and GC analysis) was obtained by washing with a sodium hydroxide solution, drying with sodium sulfate, and performing vacuum distillation.

CuS (Johnson Matthey, 97% pure), Cu_2S (Johnson Matthey, 99.99% pure), $CuSO_4 \cdot 5H_2O$ (Janssen, *p.a.*), and ZnS (Merck, *Patinal*) were used as supplied.

Catalyst Preparation

All catalysts were prepared by homogeneous deposition precipitation of copper nitrate trihydrate (Merck, >99.5% pure) and zinc nitrate hexahydrate (Janssen, >98% pure) onto Shell S980A silica (75–125 μm) according to the method described by Van de Grift *et al.* (55). Two catalysts were used: CS15 (15 wt% copper on silica) and CZS1510 (15 wt% copper and 9 wt% ZnO on silica).

High-Pressure Hydrogenolysis

Activity and deactivation experiments were performed in a high-pressure liquid-flow setup described in (6). In an autoclave, hydrogen and methyl ester feed were dissolved in octane at elevated pressure and flowed by means of a HPLC pump into a fixed-bed reactor. The apparatus allowed near-instantaneous addition of the sulfur compound from a second storage vessel and HPLC pump without changing the ester and hydrogen concentration. Along with the sulfur compound, an inert alkane tracer was added, to check for plug flow and delay of the system. Internal and external mass- or heat-transfer limitations were found to be absent by calculating the Carberry number, Wheeler–Weisz modulus, Prater number, Prater film number, and Arrhenius number, and checking their values against the criteria given in (56).

The experiments were carried out with 200 mg of catalyst. Preceding the experiment, the catalyst was calcined for 12 h at 750 K in a flow of 120 ml min^{-1} dry air. Reduction was performed in a flow of 120 ml min^{-1} hydrogen (Praxair, 99.999% pure) for 1 h at 600 K. In both cases, a heating rate of 72 K h^{-1} was used. Regeneration treatments were performed in a similar way.

During the experiment, a liquid flow rate of 0.8 ml min^{-1} of a 0.01 mol L^{-1} methyl palmitate solution in octane was passed over the catalyst ($W/F = 2500$ kg_{cat} s mol^{-1}). Preceding the experiment, the reaction mixture was saturated with hydrogen at a pressure of 8.0 MPa (Praxair, 99.999% pure) and a temperature of 293 K unless otherwise indicated.

Some experiments were conducted using deuterium (Norsk Hydro) instead of hydrogen. In this case, the catalyst received a standard reduction treatment (in hydrogen) followed by treatment in deuterium for 2 h at the temperature of reduction. Subsequently, the catalyst was cooled down under a flow of deuterium to reaction temperature. Deuterium was dissolved in the reaction medium at a pressure of 4.0 MPa.

The reaction temperature was always 470 K. Selectivity for ester hydrogenolysis was not explicitly mentioned as the formation of undesirable by-products (wax esters, hydrocarbons) was usually less than 5%.

Generally, a concentration of 0.00219 mol L^{-1} (356 ppm, mol/mol) of the sulfur compound was used. In the case of $C_{16}S_2C_{16}$, half this concentration was used because two sulfur atoms are present in each molecule.

Some experiments were conducted without hydrogen to establish the role of hydrogen in the deactivation and/or adsorption process. To remove residual hydrogen after reduction, the catalyst was flushed with a solution of 0.0219 mol L^{-1} hexadecene (Aldrich, >99% pure) until no further hexadecane formation was found.

The reaction products were identified using a JEOL JMS SX/SX102A mass spectrometer, suitable for field desorption, and a HP5890 series II gas chromatograph with a 5791 series mass selective detector, using DB5 and DB-Wax capillary columns. Quantitative product analysis was performed on Carlo Erba Mega Series 6000 gas chromatographs, using J&W Scientific DB1 and DB-Wax capillary columns.

Catalyst Characterization

Detailed analysis of the catalysts applied is given in (4–6). Temperature-programmed oxidation (TPO) and temperature-programmed reduction (TPR) experiments were performed in a setup described elsewhere (57). About 16 mg of one of the model compounds (CuS, Cu_2S, ZnS, or $CuSO_4(H_2O)_5$) or about 40 mg of spent catalyst was heated at a ramp rate of 600 K h^{-1} from room temperature to 1273 K, with a 30-min dwell time. TPO was conducted in a flow of a 20 ml min^{-1} mixture of 20% O_2 (Praxair, 99.995% pure) in He (Praxair, 99.999% pure); TPR was carried out in a flow of a 20 ml min^{-1} $Ar/H_2 = 33/66$ (Praxair, 99.999% pure).

X-ray diffraction was performed on a Philips PW 1380 diffractometer, using Cu$K\alpha$ radiation (0.15418 nm). Crystallite sizes were calculated using the Scherrer equation with a shape factor of 1. The linewidth was corrected for instrumental broadening.

RESULTS AND DISCUSSION

Alkyl Thiol Deactivation

In Fig. 1, the deactivation profile of a CZS1510 catalyst is shown. At $t = 0$ min, octadecanethiol and the tetradecane tracer are added to the reaction mixture. At $t = 30$ min, breakthrough of the tracer is observed. The delay in tracer breakthrough is largely caused by dead volume in the mixing and sampling lines. The concentration front of the tracer, however, is quite steep on the time scale of the experiment; within one sample interval, over 90% of the inlet concentration is reached.

Two decomposition products of octadecanethiol are found: octadecane and to a lesser extent a mixture of octadecenes (1-, 2-, and 3-octadecenes and their cis–trans isomers). After $t = 100$ min, octadecanethiol breakthrough is observed. Also, small amounts of dioctadecyl sulfide were formed. Similar experiments with only the silica carrier, however, also showed the formation of dioctadecyl sulfide in the same concentration range. Therefore, the formation of the sulfide is not necessarily related to the active phase.

Deactivation of the unpromoted CS15 catalyst by octadecanethiol (Fig. 2) shows the same pattern as that found for the zinc-promoted CZS1510 catalyst. However, for CS15, deactivation is somewhat faster and octadecanethiol breakthrough occurred at 80 min (versus 120 min for CZS1510). It is likely, therefore, that zinc to some extent guards the promoted catalyst by preferentially adsorbing sulfur as was discussed in the Introduction. Additionally, the lower copper surface area of the unpromoted sample may have been of influence. However, since the difference is only about 16% (15.2 $m^2\ g^{-1}$ for CS15 and 17.7 $m^2\ g^{-1}$ for CZS1510 [see (4)]) this cannot account for the difference in thiol breakthrough time by itself.

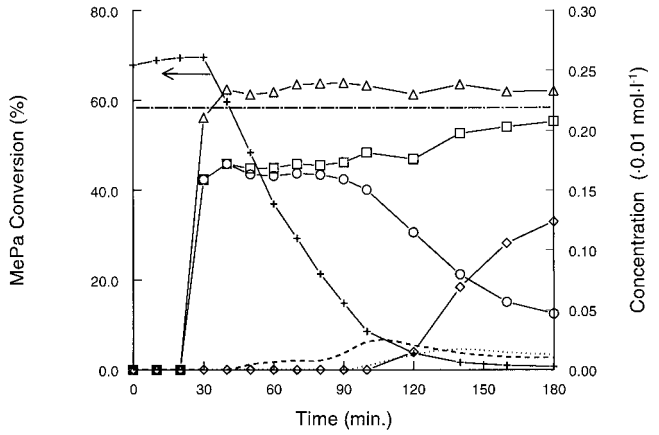

FIG. 1. Deactivation of a CZS1510 (15 wt% Cu and 9 wt% ZnO on SiO_2) catalyst using octadecanethiol. Left axis: +, methyl palmitate conversion. Right axis: △, tetradecane tracer; □, sum of octadecanethiol, octadecane, and octadecenes; ○, octadecane; ◇, octadecanethiol; ----------, octadecenes; ....., dioctadecyl sulfide; - - - - - - -, initial octadecanethiol concentration.

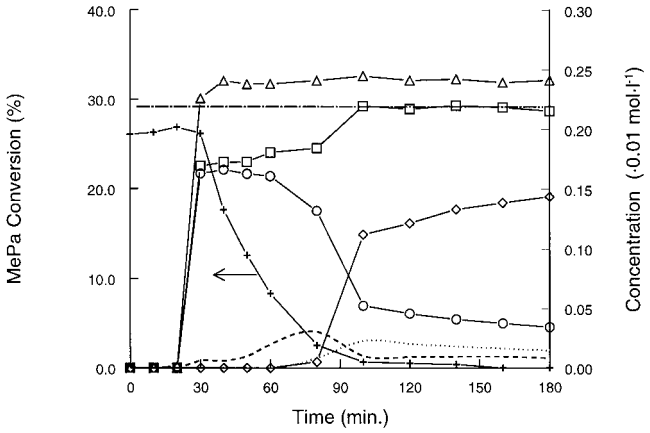

FIG. 2. Deactivation of a CS15 (15 wt% Cu on silica) catalyst using octadecanethiol. Left axis: +, methyl palmitate conversion. Right axis: △, tetradecane tracer; □, sum of octadecanethiol, octadecane, and octadecenes; ○, octadecane; ◇, octadecanethiol; ----------, octadecenes; ....., dioctadecyl sulfide; - - - - - - -, initial octadecanethiol concentration.

In Figs. 1 and 2, the sum of octadecanethiol and products thereof (octadecane and octadecenes) does not equal the initial octadecanethiol concentration. This suggests some form of accumulation of hydrocarbon moieties on the catalyst. This is most apparent for the CZS1510 catalyst; for CS15, the sum of octadecanethiol and reaction products reaches initial thiol concentration rapidly after breakthrough of octadecanethiol (see Fig. 2).

n-Alkyl Thiol Decomposition

Bourne *et al.* reported that, during deactivation of nickel catalysts by thiols, the alkyl chains remain on the catalyst. No clear distinction, however, could be made as to whether the alkyl chains remain on the catalyst as adsorbed thiols or as carbonaceous residues (58). Accumulation of non-dissociated *n*-alkane thiols on noble metals like gold is well documented. This process is also referred to as self-assembling monolayers ((59) and references therein). As was mentioned in the introduction, the remaining alkyl chains may cause catalyst deactivation as well, the extent of deactivation being related to the number of carbon atoms (39).

The formation of adsorbed *n*-alkyl thiols is further illustrated in Fig. 3. For 1 h, the catalyst is deactivated using octadecanethiol along with the tetradecane tracer. Subsequently, octadecanethiol is removed from the feed stream,

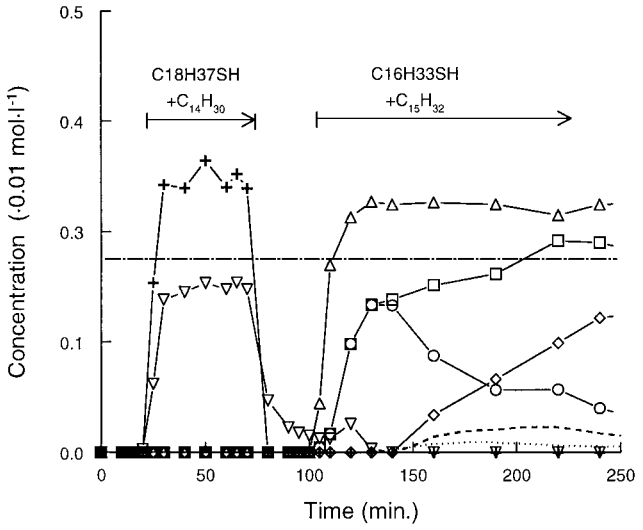

FIG. 3. Thiol decomposition on a CZS1510 catalyst using octadecanethiol and hexadecanethiol. +, tetradecane tracer; ▽, octadecane; △, pentadecane tracer; □, C_{16} balance (see text); ○, hexadecane; ◇, hexadecanethiol; ----------, hexadecenes; ....., dihexadecyl sulfide; - · - · - · -, initial hexadecanethiol and octadecanethiol concentration. Hydrogen pressure: 8.0 MPa; no fatty methyl ester is added.

and octane is passed over the catalyst for 30 min. This results in a rapid decrease in tetradecane tracer concentration and—a somewhat more gradual—decrease of octadecane (a product of the decomposition of octadecanethiol). Subsequently, hexadecanethiol is passed over the catalyst, with pentadecane as the tracer. At $t = 100$ min, breakthrough of the pentadecane tracer is observed. Remarkably, additional octadecane desorption is observed with a maximum at $t = 120$ min. Since this is a decomposition product of octadecanethiol, it is indicative for the presence of octadecyl fragments on the catalyst, either adsorbed as alkyl fragments or as alkyl thiols.

Adsorption of the alkane tracers is negligibly small during our experiments; the concentration front is always quite steep and, after removal from the reaction mixture, no desorption of the alkane is observed (see, for instance, Fig. 3). In view of this, it is likely that the alkyl fragments left on the catalyst during thiol adsorption are still bound to sulfur.

This effect is less apparent on the unpromoted CS15 catalyst (not shown here). This and the fact that Sexton and Nyberg (60) reported that thiols readily decompose on Cu(100) surfaces at temperatures below our reaction temperature may indicate that the adsorbed alkyl thiols are stabilized by the zinc constituent of the catalyst.

Mechanism of Thiol Decomposition

As is clear from Figs. 1 and 2, alkanes and alkenes are formed during thiol decomposition on both the unpromoted and the zinc-promoted catalyst. The following steps could be postulated to describe the product distribution:

$$C_{18}H_{37}SH + * \rightarrow C_{18}H_{38} + S^*; \quad [1]$$

$$C_{18}H_{37}SH + * \rightarrow C_{18}H_{36} + S^* + H_2; \quad [2]$$

$$C_{18}H_{36} + H_2 \rightarrow C_{18}H_{38}. \quad [3]$$

At first sight, incorporation of [1] does not seem necessary to allow for the formation of both alkanes and alkenes; it is well known that double-bond hydrogenation occurs over copper catalysts under hydrogenolysis conditions (7); i.e., alkanes could be formed by the hydrogenation of alkenes. Furthermore, it was proposed that decomposition of thiols over nickel catalysts proceeds via the formation of 1-alkenes (58).

To gain insight into these reaction steps, experiments *without hydrogen* were performed; i.e., reaction [3] is inhibited. The fact that the catalyst is pretreated in hydrogen preceding the experiment complicates the experimental procedure somewhat. To overcome the problem of residual hydrogen after catalyst reduction, a solution of 0.00219 mol L^{-1} of 1-octadecene is passed over the catalyst until double-bond hydrogenation is no longer observed. Subsequently, hexadecanethiol (0.00219 mol L^{-1}) is added to this mixture. The resulting breakthrough curve obtained with the CZS1510 catalyst is shown in Fig. 4.

During the experiment, hexadecanethiol decomposition results in the formation of both hexadecane and a mixture of hexadecenes (like 2-hexadecene, 3-hexadecene, and cis–trans isomers thereof). This provides strong evidence that at least two concurrent thiol decomposition mechanisms take place, one leading to the formation of an alkane and the other to (a mixture of) alkenes. It also demonstrates

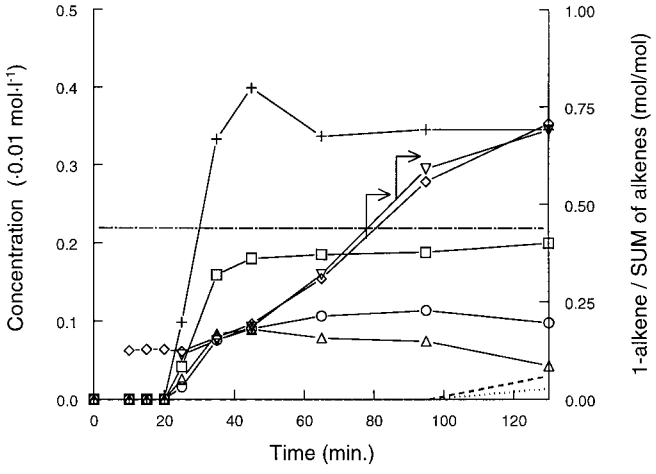

FIG. 4. Decomposition of hexadecanethiol over the CZS1510 catalyst. +, tetradecane tracer; □, C_{16} balance (see text); ○, hexadecane; △, hexadecenes; ----------, hexadecanethiol; ....., dihexadecyl sulfide; - · - · - · -, initial hexadecanethiol concentration; ▽, 1-hexadecene concentration divided by the sum of all C_{16} alkenes (see text); ◇, 1-octadecene divided by the sum of all C_{18} alkenes (see text).

that essentially no carbon deposition occurred during 1-octadecene pretreatment.

The reverse of reaction [3] may, in principle, account for the formation of hexadecenes, rather than direct thiol dissociation. However, dehydrogenation of the alkane tracers is never observed. It seems likely, therefore, that dehydrogenation of alkanes (reverse reaction of [3]) can be ruled out under the conditions applied here. Conversely, hydrogenation of alkenes by hydrogen stemming from reaction [2] is unlikely as no octadecane formation is observed from octadecene added to the reaction mixture (see below).

The relative amount of 1-hexadecene increases at the expense of other alkenes during the experiment, probably as a result of deactivation of the active phase. This is also illustrated in Fig. 4, where the amount of 1-hexadecene divided by all C_{16} alkenes is shown. The fact that a similar trend is observed for octadecenes, formed from 1-octadecene (which is added to the reaction mixture), indicates alkenes are formed as 1-alkene and that the double bonds undergo positional (and cis–trans) isomerization over the catalyst. As catalyst deactivation proceeds, positional isomerization becomes less evident and preferentially the 1-alkene is found.

A somewhat more detailed mechanism of thiol decomposition is shown in Fig. 5. The initial step consists of coordination of the thiol to the surface. As was discussed before, thiol dissociation both to the corresponding 1-alkene and to the alkane occurs under our reaction conditions, in contrast to thiol decomposition over nickel catalysts, which is suggested to proceed toward the 1-alkene only (58). 1-Alkene formation may, for instance, occur via β-hydrogen abstraction (Fig. 5, reaction [1]). When active sites are still available, the 1-alkene may be either hydrogenated to alkanes (reaction [3]) or undergo internal isomerizations. The path to alkanes (reaction [2]) is somewhat more complicated since it requires the addition of hydrogen to the α-carbon atom. This may occur by hydrogenation

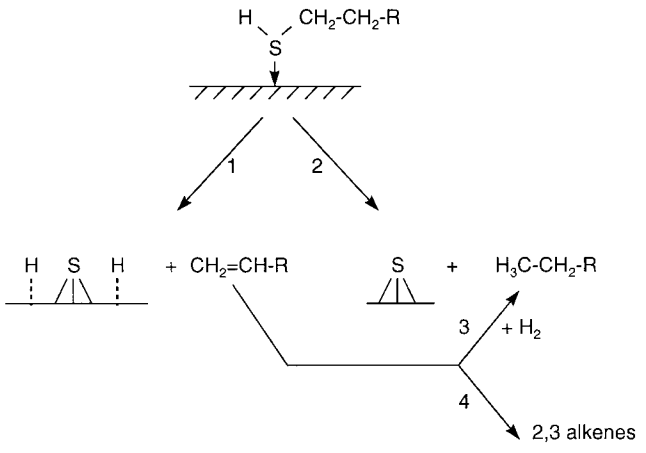

FIG. 5. Schematic representation of the decomposition of thiols.

with adsorbed hydrogen or shift of the hydrogen from the adsorbed sulfur.

As was mentioned already, under conditions with hydrogen present, the main products of the decomposition of thiols are the corresponding alkanes, whereas without hydrogen both alkanes and alkenes were formed. To elucidate which of the thiol decomposition pathways shown in Fig. 5 predominates when hydrogen is present—direct decomposition to the corresponding alkanes (step 2) or decomposition to alkenes with subsequent hydrogenation (steps 1–3)—some preliminary deuterium labeling studies were conducted. The experiments were performed with a CS15 catalyst, deuterium instead of hydrogen and hexadecanethiol. Samples were taken at incomplete catalyst deactivation (i.e., still considerable residual hydrogenation/deuteration activity left). In this case, within experimental limitations, only alkanes containing zero or one deuterium atom was found. This implies that, to a large extent, hydrogen from the thiol group (*RS***H**) is built into the corresponding alkane product (Fig. 5, step 2). Furthermore, little or no alkenes are formed and subsequently hydrogenated toward alkanes (Fig. 5, steps 1 and 3). Hence, alkanes are not formed through hydrogenation of alkenes under these conditions. This indicates that reaction 1 in Fig. 5 is strongly inhibited when hydrogen (deuterium) is present in the reaction mixture. At prolonged exposure times, higher deuterium exchanged (e.g., containing two or three deuterium) alkanes and alkenes were observed, indicating that on a (partially) deactivated copper surface the formation of alkenes does proceed under conditions with hydrogen present.

Influence of the Nature of the Sulfur-Containing Molecule

In Fig. 6, deactivation of the zinc-promoted CZS1510 catalyst with all tested sulfur-containing molecules is shown. The initial conversion level is normalized at 1 (initial turnover frequencies: CZS15, $TOF_0 = 0.95$ mmol mol_{Cu}^{-1} s^{-1}; CSZ1510, $TOF_0 =$ 1.90 mmol mol_{Cu}^{-1} s^{-1}). It is clear that rapid deactivation is observed for all sulfur compounds tested.

Similar deactivation profiles are found for the CS15 catalyst (see Fig. 7). Compared to the CZS1510 catalyst, a somewhat more rapid catalyst deactivation is observed for most sulfur-containing molecules. This is also apparent from Fig. 8, where half-life times of the catalyst are shown. Depending on the type of sulfur compound, zinc addition can more than double the catalyst lifetime at the applied loading. This could be due to the already mentioned differences in the free energies of formation of zinc and copper sulfides; zinc sulfide is thermodynamically more stable than copper sulfide. Alternatively, zinc oxide may also simply serve as an additional adsorption surface. Increased copper dispersion of the zinc-promoted catalyst compared to the unpromoted sample is not the reason for the observed

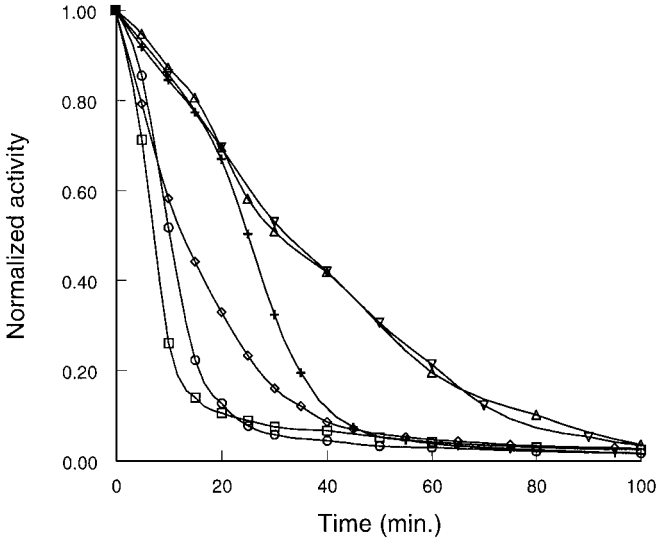

FIG. 6. Deactivation of the CZS1510 catalyst. Sulfur-containing molecule: ▽, octadecanethiol; △, dihexadecyl disulfide; ○, dihexadecyl sulfide; □, dibenzothiophene; ◇, methyl *p*-toluenesulfonate; +, benzyl isothiocyanate. Conditions as indicated in Experimental.

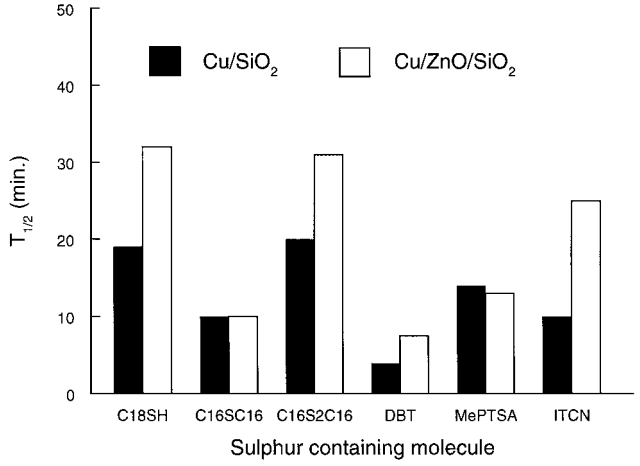

FIG. 8. Half-life time values for CS15 and CZS1510 catalysts for several sulfur-containing molecules. Conditions as indicated in Experimental.

phenomena as the metal surface areas, determined by N_2O chemisorption, differ only by 16% (see above).

Evidently, the nature of the sulfur-containing molecule determines the rate of deactivation of the catalyst. Octadecanethiol and dihexadecyl disulfide deactivate the slowest, both for the unpromoted and zinc-promoted catalyst. This can be explained by fast decomposition of the disulfide into the corresponding thiol over the catalyst. Consequently, predominantly hexadecanethiol is observed in the reaction mixture. Furthermore, hexadecanethiol breakthrough is observed in a way similar to that during experiments with octadecanethiol. One may assume, therefore, that disulfides decompose into the corresponding thiols under our reaction conditions. This is in agreement with experiments on nickel catalysts, where thiols and disulfides were reported to show similar deactivation behavior (58).

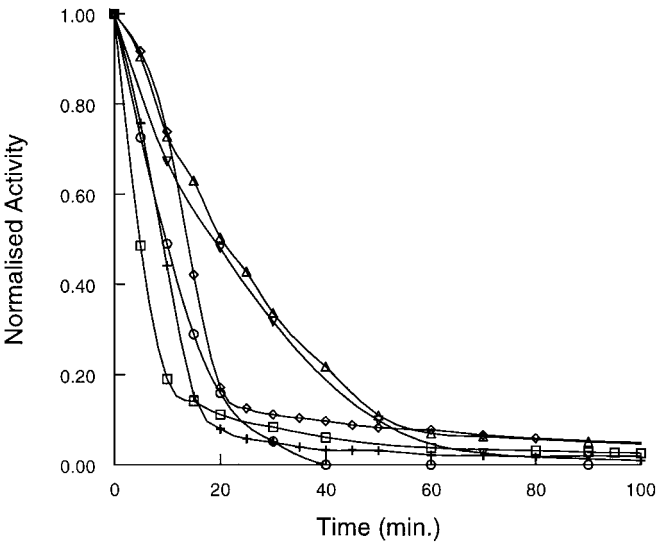

FIG. 7. Deactivation of the CS15 catalyst. Sulfur-containing molecule: ▽, octadecanethiol; △, dihexadecyl disulfide; ○, dihexadecyl sulfide; □, dibenzothiophene; ◇, methyl *p*-toluenesulfonate; +, benzyl isothiocyanate. Conditions as indicated in Experimental.

Residual sulfur oxides resulting from methyl *p*-toluene sulfonate adsorption and decomposition will probably decompose, in turn, on copper into adsorbed sulfur and oxygen (see (61)), the latter species being converted to water at the applied conditions.

The fastest deactivation rate is observed for dibenzothiophene and dihexadecyl sulfide. At least three explanations may be proposed: (i) the size of the (adsorbed) sulfur-containing molecules, (ii) the fact that these molecules require hydrogenation preceding desulfurization, and (iii) pre ferential adsorption at sites with high hydrogenolysis activity.

Dibenzothiophene is among the bulkiest molecules tested in our studies. As was discussed above, there is evidence for adsorbed alkyl thiol fragments in octadecanethiol deactivation. It is interesting to assess whether (fragments of) the dibenzothiophene molecules reside on the catalyst surface, shielding more than one active site after adsorption.

Catalyst Deactivation by Dibenzothiophene and Dihexadecyl Sulfide

The breakthrough curve of dibenzothiophene over a CS15 catalyst is shown in Fig. 9. The decomposition products of dibenzothiophene are cyclohexylbenzene and biphenyl. These products and, after breakthrough, dibenzothiophene add up nearly instantaneously to the initial amount of dibenzothiophene; i.e., no fragments other than

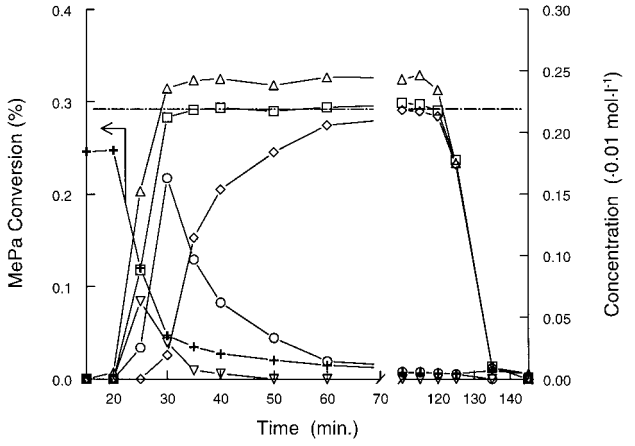

FIG. 9. Deactivation of a CZS1510 catalyst using dibenzothiophene. Left axis: +, methyl palmitate conversion. Right axis: △, tetradecane tracer; ◇, dibenzothiophene; ○, biphenyl; ▽, cyclohexylbenzene; □, balance (see text). Note the axis break and scale change.

sulfur itself remain at the catalyst surface. A similar response, with the same decomposition products, is found for the zinc-promoted catalyst. It can be assumed, therefore, that remaining fragments of the dibenzothiophene molecule do not cause the relatively fast catalyst deactivation observed.

To evaluate the influence of hydrogen on the desulfurization rate of dibenzothiophene and dihexadecyl sulfide, breakthrough experiments both in the presence and absence of hydrogen are shown in Fig. 10. It is clear that the hydrogen pressure has a profound effect on the sulfur uptake of the catalyst for both sulfur-containing molecules shown here.

In the case of the sulfide and in the absence of hydrogen, only hexadecene is detected during the entire experiment, indicative for sulfur decomposition in the absence of hydrogen according to, for instance,

$$(C_{16}H_{33})_2S \rightarrow 2C_{16}H_{32} + S_{ad} + 2H_{ad}. \qquad [4]$$

In the presence of hydrogen, both hexadecane and hexadecene in near equal amounts are formed.

In the similar case for dibenzothiophene, biphenyl, but no cyclohexyl benzene, is found in the absence of hydrogen. Although it was attempted to remove hydrogen from the catalyst using 1-octadecene preceding these two experiments and no hydrogen is present in the reaction mixture, apparently some source of hydrogen is present in the catalyst (perhaps from coke formation), making it possible to form biphenyl from dibenzothiophene:

$$C_{12}H_8S + H_2 \rightarrow C_{12}H_{10} + S_{ad}. \qquad [5]$$

It is clear from Fig. 10, however, that the presence of hydrogen significantly enhances the amount of sulfur adsorbed for both dihexadecyl sulfide and dibenzothiophene. Furthermore, dibenzothiophene obviously requires hydrogenation for desulfurization.

The surface coverage for all sulfur-containing molecules is shown in Table 1, except for benzyl isothiocyanate as the decomposition product of this compound could not be detected using GC analysis. The values in Table 1 were calculated by dividing the amount of sulfur adsorbed by the amount of copper atoms in the catalyst surface, taken from (4). Both values calculated at the moment of breakthrough of the sulfur compound and at the end of the experiment are reported. Also, the ratio of concentrations entering and leaving the catalyst at the end of the experiment is reported, which expresses whether the catalyst still adsorbs sulfur at the end of the experiment. If this value ($C_{s,f}/C_{s,i}$) is smaller

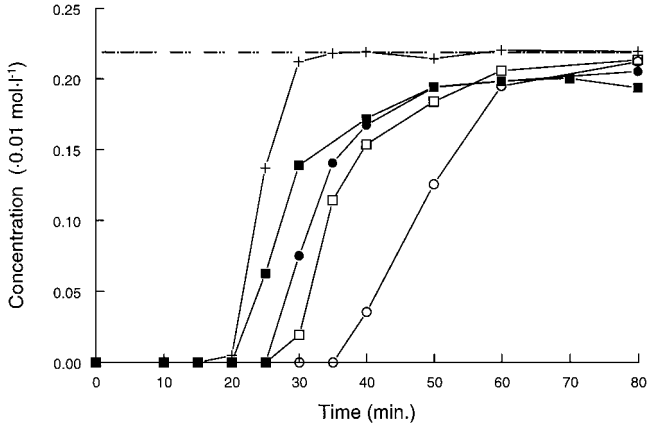

FIG. 10. The influence of hydrogen pressure on the breakthrough of sulfur-containing molecules over a CS15 catalyst. Hydrogen pressure: open symbols, 8.0 MPa; closed symbols, 0.0 MPa. +, tetradecane tracer concentration; ○, ●, dihexadecyl sulfide; □, ■, dibenzothiophene. Other conditions as indicated in Experimental.

TABLE 1

Amount of Absorbed Sulfur at Breakthrough of Sulfur-Containing Molecule and at the End of the Experiment

S-Containing molecule	Catalyst	No. of monolayers at breakthrough	No. of monolayers at end of expt.	$C_{s,f}/C_{s,i}$
$C_{18}SH$	CS15	0.31	0.58	0.65
	CZS1510	0.48	0.64	0.60
$C_{16}SSC_{16}$	CS15	0.27	0.51	0.31
	CZS1510	0.42	0.64	0.40
$C_{16}SC_{16}$	CS15	0.09	0.15	1.0
	CZS1510	0.08	0.12	1.0
DBT	CS15	0.06	0.07	1.0
	CZS1510	0.07	0.08	1.0
MePTSA	CS15	0.12	0.41	0.71
	CZS1510	0.20	0.65	0.31

Note. $C_{s,f}$ = concentration of sulfur-containing molecule at the end of reactor at the end of experiment; $C_{s,i}$ = initial sulfur concentration.

than 1, sulfur is still being adsorbed and higher surface coverage is to be expected after prolonged exposure to the sulfur compound.

Sulfur Surface Coverages

As is clear from Table 1, the maximum surface coverage found for dibenzothiophene and dihexadecyl sulfide is quite low. Since near-complete catalyst deactivation is observed at this low surface coverage, it appears that sulfur is deposited in a structured and dispersed way on the catalyst surface by these compounds. Combined with the observation that dibenzothiophene requires hydrogenation activity (reaction [5]), and that the decomposition of dihexadecyl sulfide is considerably increased by the presence of hydrogen, it can be concluded that desulfurization of these molecules preferentially proceeds over an ensemble of copper atoms and is favored by hydrogenation activity. After sulfur is adsorbed at these sites, all the surrounding atoms in the ensemble become unsuitable for both ester hydrogenolysis and decomposition of the sulfur-containing molecule.

Similar results are described by Bourne *et al.* (58) for nickel catalysts. They report that, in contrast to thiols, thiophene decomposition requires the adsorption of the molecule on a number of metal atoms, resulting in sulfur deposition on the catalyst surface in a dispersed fashion (i.e., in the vicinity of an adsorbed thiophene molecule, no consecutive adsorption can occur). Using a simple model, they substantiate that, after adsorption of sulfur on a nickel site, between four and eight (depending on the crystal face) of the neighboring nickel atoms are no longer capable of acting as adsorption sites for another thiophene molecule. This would result in a maximum nickel surface coverage of about 25%. The surface coverage obtained after dibenzothiophene adsorption on CZS1510 and CS15 catalysts, however, is even much lower (6–8%). This suggests that in our case even more neighboring sites are incapable of consecutive adsorption of dibenzothiophene. In view of the differences in molecular size of thiophene and dibenzothiophene, this is not unlikely. The more so since it is likely that (dibenzo)thiophene adsorbs (nearly) parallel to the copper-metal surface as shown for thiophene on Ni(110) (see, e.g., (62)) and for DBT on fully sulfided alumina-supported Co/Mo and Ni/Mo catalysts (63). To these findings, we may add the already discussed importance of the hydrogenation activity for thiophenes and dialkyl sulfides. The fact that neighboring metal atoms are no longer available for sulfur adsorption for these molecules may well be ascribed to the decreased ability to hydrogenate the sulfur compounds.

While Bourne *et al.* describe the effect on neighboring atoms in terms of steric effects, others focus on electronic effects; some authors propose the strong electronegativity of adsorbed sulfur to cause rapid deactivation of nickel catalysts (43, 44). At the low coverages reported here for copper catalysts deactivated by, for instance, dibenzothiophene, long-range electronic effects are less likely. Lang and Williams, for instance, conclude on the basis of charge density calculations that electronic effects on metals are very much limited to the site poisoned by adatoms (64).

The fact that copper-based catalysts are deactivated at very low sulfur surface coverage implies that the ester hydrogenolysis reaction proceeds on an ensemble of (copper) atoms, in agreement with (65). An alternative explanation for the rapid deactivation of CZS1510 and CS15 upon the addition of dibenzothiophene and dihexadecyl sulfide could be that these sulfur-containing molecules cause preferential sulfur adsorption at sites with high hydrogenolysis activity, causing a rapid ester hydrogenolysis activity loss. In view of the low final surface coverage, however, this is not likely. After catalyst deactivation, further sulfur deposition would be expected at residual, though less active, copper sites. Eventually, this would result in a sulfur surface coverage approaching $\theta = 0.5$ (see below), which was not observed (Table 1).

The largest sulfur coverage is observed for octadecanethiol. Breakthrough occurs at $\theta = 0.3$ and $\theta = 0.5$ for the unpromoted and zinc-promoted catalyst, respectively. This is in agreement with the single-crystal studies, where a maximum sulfur surface coverage of $\theta = 0.5$ is reported for most crystal faces (33, 36). At the end of the experiment, a surface coverage slightly above $\theta = 0.5$ is found. The fact that the initial octadecanethiol concentration is not reached at this point indicates that, after prolonged exposure to this sulfur compound, a higher theoretical surface coverage can be obtained. In view of the proposed maximum surface coverage of $\theta = 0.5$, this suggests slow diffusion of sulfur into the bulk phase or in the case of the zinc-promoted catalyst, a contribution to the sulfur uptake of the catalyst by ZnO. Again, quite similar trends are observed for octadecanethiol and octadecyl disulfide, in agreement with the suggestion that the disulfide readily decomposes to the thiol under reaction conditions.

The results presented in Table 1 quite conclusively demonstrate that the deactivation of the CS15 and CZS1510 catalysts primarily takes place via surface sulfidation for all sulfur-containing molecules tested, resulting in rapid catalyst deactivation. After prolonged exposure to the sulfur compound, bulk sulfide formation becomes apparent. The formation of bulk sulfide, however, is not in any way prolonging catalyst life; no significant remaining ester hydrogenolysis activity is observed when bulk sulfide formation becomes observable. However, bulk sulfide formation and additional scavenging of sulfur by zinc oxide in the deactivated catalyst could contribute to prolonged catalyst life as more sulfur can be trapped in the upper part of the catalyst bed, thus preventing sulfur reaching the downstream catalyst load.

Catalyst Regeneration

Regeneration of the deactivated catalysts by hydrogen treatment at elevated temperature was attempted after both partial and complete deactivation by various sulfur-containing compounds. Even though the treated catalyst adsorbs additional sulfur and therefore some sulfur must have been removed, the initial activity of the catalyst cannot be restored upon treatment in hydrogen at 600 K.

To further investigate the regeneration process, temperature-programmed oxidation and reduction experiments were performed. The evolved products, H_2S or SO_2, can be identified using UV–vis absorption spectroscopy (57, 66).

TPR of a CZS1510 catalyst after deactivation by benzyl isothiocyanate shows some desorption of H_2S at ca. 1000 K. Treatment at 1000 K is certainly not feasible in industrial hydrogenolysis reactors and will cause extensive active-metal sintering. A comparison with TPR profiles of reference compounds demonstrates that no separate bulk CuS, Cu_2S, or $CuSO_4$ phases exist in the deactivated catalyst.

In TPO two SO_2 desorption maxima are observed for benzyl isothiocyanate deactivated CZS1510. A first maximum at $T = 580$ K is accompanied by oxygen consumption and a high-temperature peak at $T = 1050$ K by some oxygen production. Comparison of TPR and TPO profiles of deactivated catalysts with those of pure CuS, Cu_2S, $CuSO_4$, and ZnS reveals that none of the separate bulk phases are formed. Also, in view of the low sulfur uptake by the catalysts reported in this paper, surface sulfides most likely predominate.

Some authors report the regeneration of sulfur-deactivated metal catalysts using oxidation–reduction cycles (47, 48). In the TPO profile of the deactivated catalyst, some oxygen consumption and release of SO_2 is detected at 580 K. If this were due to copper sulfate formation, the TPR of pure $CuSO_4$ indicates that reduction at 600 K would result in the decomposition of this phase. After oxidation in dry air at 750 K and subsequent reduction at 600 K, the deactivated catalyst showed no activity. This could be due to the fact that sulfur remains on the surface of the catalyst or to copper-metal sintering.

The X-ray diffraction pattern of a $Cu/ZnO/SiO_2$ catalyst deactivated by benzyl isothiocyanate revealed only three broad peaks at $2\theta = 42.1$, 47.2, and 48.7° which could not be ascribed to reference materials like copper, zinc oxide, CuS, Cu_2S, $CuSO_4$, ZnS, or $ZnSO_4$, in agreement with the TPR and TPO results. The particle size, calculated for the peak at 47.2° using the simple Scherrer equation, is 4.5 nm, somewhat larger than the copper particle size of 3.5 nm reported earlier for nondeactivated $Cu/ZnO/SiO_2$ (4) and Cu/SiO_2 (55). This moderately increased particle diameter cannot account for the total loss of activity observed. After oxidizing at 750 K and reduction at 600 K, XRD reveals broad peaks at $2\theta = 43.3$, 44.3, and 74.2°, attributable to metallic copper with a particle size of 4.3 nm. Again, loss of metal dispersion during the oxidation–reduction treatment is apparently not decisive.

In conclusion, catalyst reactivation proves impossible by conventional means.

CONCLUSIONS

Deactivation of silica-supported copper catalysts is rapid during exposure to all of the sulfur compounds tested. The type of sulfur compound strongly influences the rate of deactivation. It increases in the following order: octadecanethiol ≈ dihexadecyl disulfide < benzyl isothiocyanate < methyl *p*-toluenesulfonate < dihexadecyl sulfide < dibenzothiophene. The rapid deactivation is caused by the fact that sulfur is quantitatively removed from the reaction mixture and because mainly surface sulfides rather than bulk sulfides are formed under ester hydrogenolysis conditions.

The addition of zinc to the catalyst results in increased catalyst life up to a factor of ca. 2 for most sulfur compounds tested. This is probably due to the thermodynamic stability of ZnS compared to that of copper sulfides, although no bulk ZnS phase could be identified by either temperature-programmed techniques or XRD.

During exposure to octadecanethiol, evidence was obtained for adsorption without C–S bond scission. Decomposition of the adsorbed thiols proceeds either to the corresponding alkane or 1-alkene, both with or without hydrogen in the feed. After desulfurization, hydrogenation or isomerization (positional and cis–trans) of the latter may occur. However, experiments with deuterium indicate that the low amount of alkanes found in the reaction mixture in the presence of H_2 (or D_2) is not due to secondary alkene hydrogenation but rather a consequence of inhibition of the alkene formation reaction pathway.

Dihexadecyl disulfide rapidly decomposes to the corresponding thiol, resulting in sulfur deposition and catalyst deactivation similar to that of the thiol. Hydrogen and hydrogenation activity is not required for the desulfurization of these compounds.

The maximum surface coverage obtained after catalyst deactivation with dibenzothiophene and dihexadecyl sulfide (the sulfur compounds that cause fastest deactivation) is significantly lower than the maximum coverage of $\theta = 0.5$, reported for most copper crystal faces. Decomposition of these molecules preferentially proceeds on copper ensembles with hydrogenation activity. This results in sulfur being deposited on the surface in a structured and dispersed fashion, causing nearly complete catalyst deactivation even at a sulfur surface coverage of 0.07. These results imply that desulfurization of both sulfur compounds as well as the ester hydrogenolysis reaction itself requires an ensemble of copper atoms.

Catalyst activity cannot be regained for catalysts deactivated with octadecanethiol or benzyl isothiocyanate by a treatment in a hydrogen atmosphere up to 600 K. TPR and TPO results also confirm that no distinct CuS, Cu_2S, $CuSO_4$, or ZnS phase is present in the deactivated catalyst. No hydrogenolysis activity could be regained by a combined oxidation/reduction cycle either. This may be due to the presence of a thermodynamically stable surface sulfide layer.

From the TPR and TPO results, it can be concluded that sulfur is removed from the catalyst only above 1000 K under both reducing and oxidizing conditions. This temperature, however, is not feasible for commercial hydrogenolysis reactors and would certainly lead to irreversible phase changes or sintering of catalyst material.

Since surface sulfide formation predominates over bulk sulfide formation, and because catalyst regeneration is not feasible, industrial application of these catalysts requires a low-sulfur-containing feed.

In view of the differences in the deactivation behavior of the sulfur-containing molecules tested, it is required to establish the nature of the sulfur-containing molecules present in the fatty methyl ester feedstock for reliable estimation of catalyst life and reactor design.

REFERENCES

1. Kreutzer, U. R., *JAOCS* **61**(2), 343 (1984).
2. Hoyng, H. B. M., "Proceedings of the World Conference on Oleochemicals, Kuala Lumpur, Malaysia, 1990," p. 211.
3. Scheur, F. T. v. d., and Staal, L. H., *Appl. Catal.* **108**(1), 63 (1994).
4. Brands, D. S., Poels, E. K., Krieger, T. A., Makarova, O. V., Weber, C., Veer, S., and Bliek, A., *Catal. Lett.* **36**(3, 4), 175 (1996).
5. Brands, D. S., Poels, E. K., and Bliek, A., *Stud. Surf. Sci. Catal.* **101**, 1085 (1996).
6. Brands, D. S., Ph.D. thesis, University of Amsterdam, The Netherlands, 1998.
7. Voeste, T., and Buchold, H., *JAOCS* **61**(2), 350 (1984).
8. Scheur, F. T. v. d., U-A-Sai, G., and Bliek, A., *JAOCS* **72**(9), 1027 (1995).
9. Betta, R. A. D., and Ushiba, K. K., *Hydrocarbon Process.* **59**(11), 157 (1980).
10. Campbell, L. D., and Slominski, B. A., *JAOCS* **67**(2), 73 (1990).
11. Irandoust, S., and Edwardsson, J., *JAOCS* **70**(11), 1149 (1993).
12. Filip, V., Krejzlíková, I., and Zajíc, J., *Fat Sci. Technol.* **97**(2), 530 (1995).
13. Cecchi, G., Llopiz, P., Maire, Y., Porte, L., and Ucciani, E., *Rev. Fr. Corps Gras* **10**, 393 (1983).
14. Guth, H., and Grosh, W., *JAOCS* **70**(5), 513 (1993).
15. Lindh, L. A., and Dahlén, J. Å. H., *JAOCS* **66**(7), 972 (1989).
16. Scarlet, J., and McKinley, D., *Oil Fat Ind.* **9**(2), 32 (1993).
17. Kirk, R. E., and Othmer, D. F., "Encyclopaedia of Chemical Technology," Vol. 5, p. 776. Interscience Publishers Inc., New York, 1950.
18. "Ullmann's Encyclopaedia of Industrial Chemistry," 5th ed., Vol. A9, p. 572. VCH Verlagsgesellschaft, Weinheim, Germany, 1986.
19. Thomas, C. L., "Catalytic Processes and Proven Catalysts," p. 146. Academic Press, New York, 1970.
20. Wood, B. J., Isakson, W. E., and Wise, H., *Ind. Eng. Chem. Prod. Res. Dev.* **19**, 197 (1980).
21. Padley, M. B., Rochester, C. H., Hutchings, G. J., and King, F., *J. Chem. Soc., Faraday Trans.* **90**(1), 203 (1994).
22. Radovic, L. R., and Vannice, M. A., *Appl. Catal.* **29**, 1 (1987).
23. Guoyong, C., Dagang, A., and Chengyue, L., *Catal. Deact.* 539 (1991).
24. Roberts, G. W., Brown, D. M., Hsiung, T. H., and Lewnard, J. J., *Ind. Eng. Chem. Res.* **32**, 1610 (1993).
25. Chaffee, A. L., Campbell, I., and Valentine, N., *Appl. Catal.* **47**, 253 (1989).
26. Khanmamedov, T. K., Kalinkin, A. V., Kundo, N. N., and Novopashina, V. M., *React. Kinet. Catal. Lett.* **37**(1), 83 (1988).
27. Terlecki-Baricevic, A., Grbic, B., Jovanovic, D., Angelov, S., Mehandziev, D., Marinova, C., and Kirilov-Stefanov, P., *Appl. Catal.* **47**, 145 (1989).
28. Fowler, R. W., and Bartholomew, C. H., *Ind. Eng. Chem. Prod. Res. Dev.* **18**(4), 339 (1979).
29. Koritala, S. V., *JAOCS* **52**, 240 (1975).
30. Cecchi, G., Castano, J., and Ucciani, E., *Rev. Franc. Corps Gras* **10**, 443 (1980).
31. Campbell, C. T., and Koel, B. E., *Surf. Sci.* **183**, 100 (1987).
32. Shatynski, S. R., *Oxid. Met.* **11**(6), 307 (1977).
33. Oudar, J., *Catal. Rev. Sci. Eng.* **22**(2), 171 (1980).
34. Bartholomew, C. H., Agrawal, P. K., and Katzer, J. R., *Adv. Catal.* **31**, 135 (1982).
35. Benard, J., *Catal. Rev. Sci. Eng.* **3**(1), 93 (1969).
36. Petrino, P., Moya, F., and Cabané-Brouty, F., *J. Solid State Chem.* **2**, 439 (1970).
37. Rostrup-Nielsen, J. R., Anderson, J. R., and Boudart, M. (Eds.), "Catalysis Science and Technology," p. 3. Springer-Verlag, Berlin, 1984.
38. "Ullmann's Encyclopaedia of Industrial Chemistry," 5th ed., Vol. A13, p. 378. VCH Verlagsgesellschaft, Weinheim, Germany, 1986.
39. Maxted, E. B., *Adv. Catal.* **3**, 129 (1951).
40. Hutchings, G. J., King, F., Okoye, I. P., and Rochester, C. H., *Appl. Catal. A* **83**, L7 (1992).
41. Hutchings, G. J., King, F., Okoye, I. P., Padley, M. B., and Rochester, C. H., *J. Catal.* **184**, 464 (1994).
42. Hutchings, G. J., King, F., Okoye, I. P., Padley, M. B., and Rochester, C. H., *J. Catal.* **148**, 453 (1994).
43. Goodman, D. W., and Kiskinova, M., *Surf. Sci.* **105**, L265 (1981).
44. MacLaren, J. M., Vvedensky, D. D., Pendry, J. B., and Joyner, R. W., *J. Catal.* **110**, 243 (1988).
45. Bartholomew, C. H., and Katzer, J. R., "Catalyst Deactivation," p. 375. Elsevier, Amsterdam, 1980.
46. Rostrup-Nielsen, J. R., *J. Catal.* **21**, 171 (1971).
47. Aguinaga, A., and Montes, M., *Appl. Catal.* **72**, L17 (1991).
48. Aguinaga, A., and Montes, M., *Appl. Catal. A* **90**(2), 131 (1992).
49. Bonzel, H. R., *Surf. Sci.* **27**, 387 (1971).
50. Corrigan, P. J., King, R. M., and Vandiest, S. A., U.S. Patent, 4,533,684, 1985.
51. Kubersky, H. P., DE 3718352 A1, 1988.
52. Scheur, F. T. v. d., Vreeswijk, J. J., and Staal, L. H., "Proceedings of the World Conference on Oilseed Technology and Utilization, 1993," p. 453.
53. Furniss, B. S., Hannaford, A. J., Smith, P. W. G., and Tatchell, A. R., "Vogel's textbook of practical organic chemistry," 5th ed./revised, p. 1160. Addison, Wesley Longman Ltd., Halow, England, 1991.
54. Harrison, H. R., Haynes, W. M., Arthur, P., and Eisenbaum, E. J., *Chem. Ind.* 1568 (1968).
55. Grift, C. J. G. v. d., Elberse, P. A., Mulder, A., and Geus, J. W., *Appl. Catal.* **59**, 275 (1990).
56. Moulijn, J. A., Tarfaoui, A., and Kapteijn, F., *Catal. Today* **11**, 1 (1991).
57. Scheffer, B., Dekker, N. J. J., Mangnus, P. J., and Moulijn, J. A., *J. Catal.* **121**, 31 (1990).
58. Bourne, K. H., Holmes, P. D., and Pitkethly, R. C., "Proceedings, Third International Congress on Catalysis, Amsterdam, 1964," p. 1400. Wiley, New York, 1965.

59. Fenter, P., Eberhardt, A., and Eisenberger, P., *Science* **266**(5188), 1216 (1994).
60. Sexton, B. A., and Nyberg, G. L., *Surf. Sci.* **165**, 251 (1985).
61. Sellers, H., and Shustorovich, E., *J. Mol. Catal. A* **119**, 367 (1997).
62. Takata, Y., Kitajima, Y., Aga, H., Yagi, S., Asahi, T., Yokoyama, T., Tanaka, K., and Ohta, T., *Jpn. J. Appl. Phys. 1* **32**(Suppl.) **32-2**, 350 (1993).
63. Lamure-Meille, V., Schulz, E., Lemaire, M., and Vrinat, M., *Appl. Catal. A* **131**, 143 (1995).
64. Lang, N. D., and Williams, A. R., *Phys. Rev. B* **18**, 616 (1978).
65. Kohler, M. A., Cant, N. W., Wainwright, M. S., and Trimm, D. L., "Proceedings, Ninth International Congress on Catalysis, Calgary, 1988" (M. J. Phillips and M. Ternan, Eds.), Vol. 5, p. 1043. Chem. Institute of Canada, Ottawa, 1988.
66. Kijlstra, W. S., Komen, N. J., Andreini, A., Poels, E. K., and Bliek, A., *Stud. Surf. Sci. Catal.* **101**, 951 (1996).